SO_2 emissions and lifetimes derived from TROPOMI observations over India using a flux-divergence method

Yutao Chen[1,2], Ronald J. van der A[1], Jieying Ding[1], Henk Eskes[1], Jason E. Williams[1], Nicolas Theys[3], Athanasios Tsikerdekis[1], Pieternel F. Levelt[1,2,4]

[1]Royal Netherlands Meteorological Institute (KNMI), De Bilt, the Netherlands
[2]Department of Geoscience & Remote Sensing, Delft University of Technology (TUD), Delft, the Netherlands
[3]Royal Belgian Institute for Space Aeronomy (BIRA-IASB), Brussels, Belgium
[4]National Center for Atmospheric Research (NCAR), Boulder, Colorado, the United States

Correspondence to: Yutao Chen (yutao.chen@knmi.nl), Jieying Ding (jieying.ding@knmi.nl)

1.One-dimensional example of Second Order Central Difference method

To introduce the divergence calculation based on a grid scale, a one -dimensional example is illustrated here. If we aim to calculate the SO_2 divergence of grid i along the x direction, the calculation can be represented as follows:

$$D_{x(i)} = \frac{\vec{F}_{x(i+1)} - \vec{F}_{x(i-1)}}{2\Delta x}$$

$$\vec{F}_{x(i+1)} = \vec{w}_{x(i+1)} \cdot V_{x(i+1)} \qquad (1)$$

$$\vec{F}_{x(i-1)} = \vec{w}_{x(i-1)} \cdot V_{x(i-1)}$$

In this equation, $\vec{F}_{x(i)}$ denotes the flux of SO_2 in grid i along x direction, Δx is the resolution of the grid-scale data. $\vec{w}$ is the wind along x direction. V *is* SO_2 VCD. The total divergence of each grid cell is the sum of the divergence in x and y directions.

2. SO_2 chemical lifetime

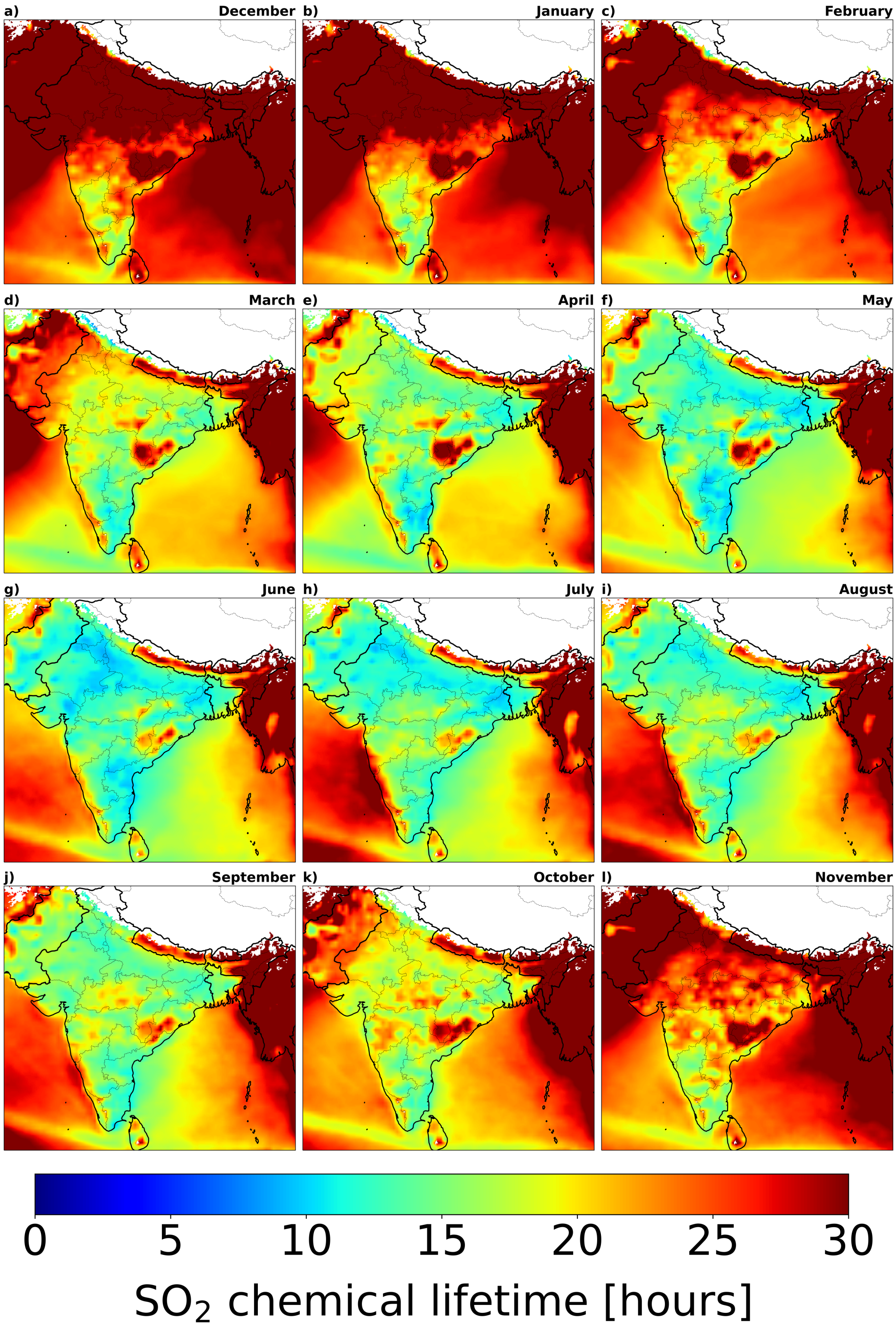

Figure S1. SO_2 monthly mean chemical lifetimes in India. The chemical lifetimes in each month are averaged within December 2018 to November 2023. The white region represents the areas with surface height above 3 km or the areas without high-quality SO_2 measurements and are not discussed in this study.

3. SO_2 dry deposition lifetime

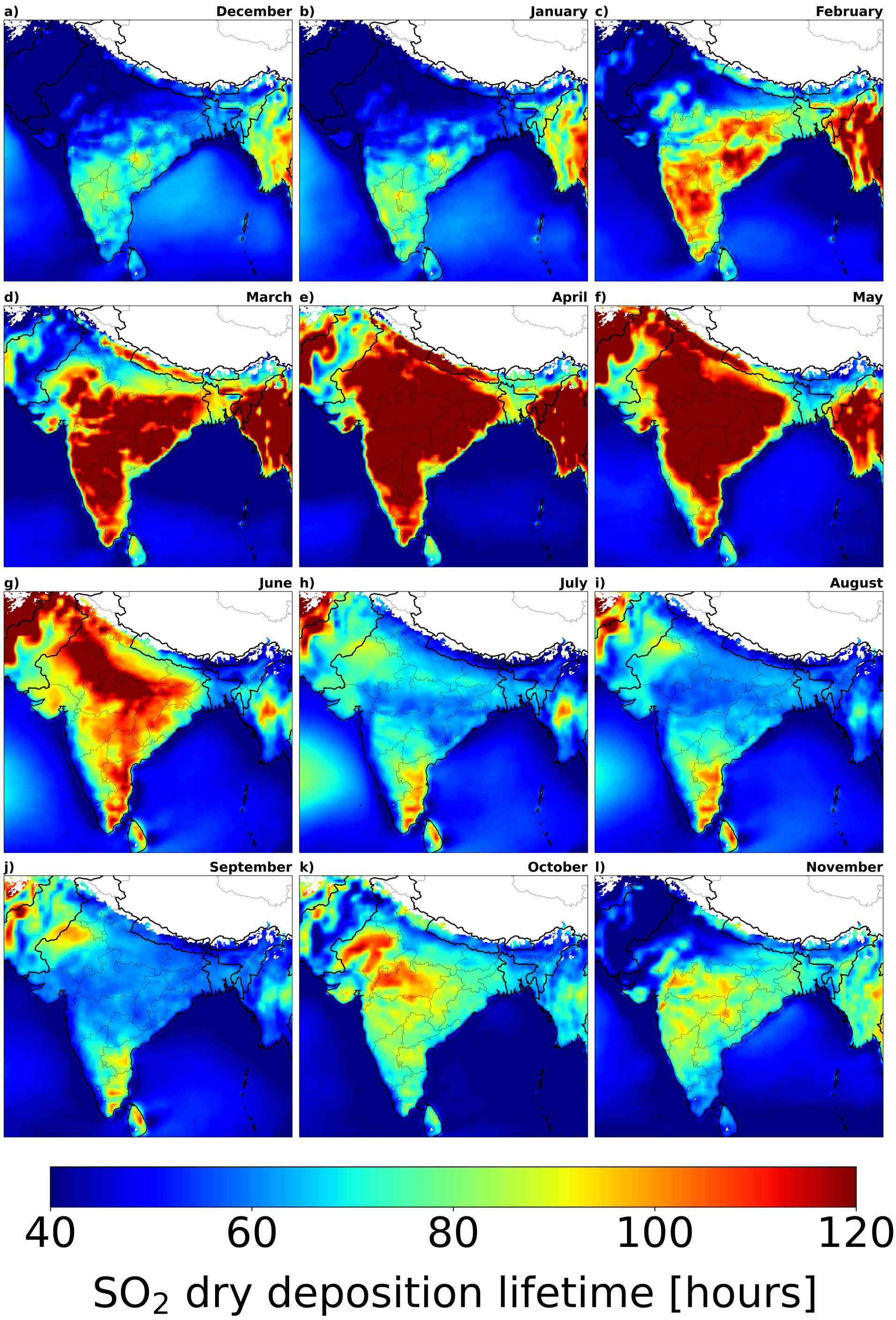

Figure S2. SO_2 monthly mean dry deposition lifetime in India. The dry deposition lifetime in each month is averaged over December 2018 to November 2023. The white region represents the areas with surface height above 3 km or the areas without high-quality SO2 measurements and are not discussed in this study.

4. SO_2 effective lifetime

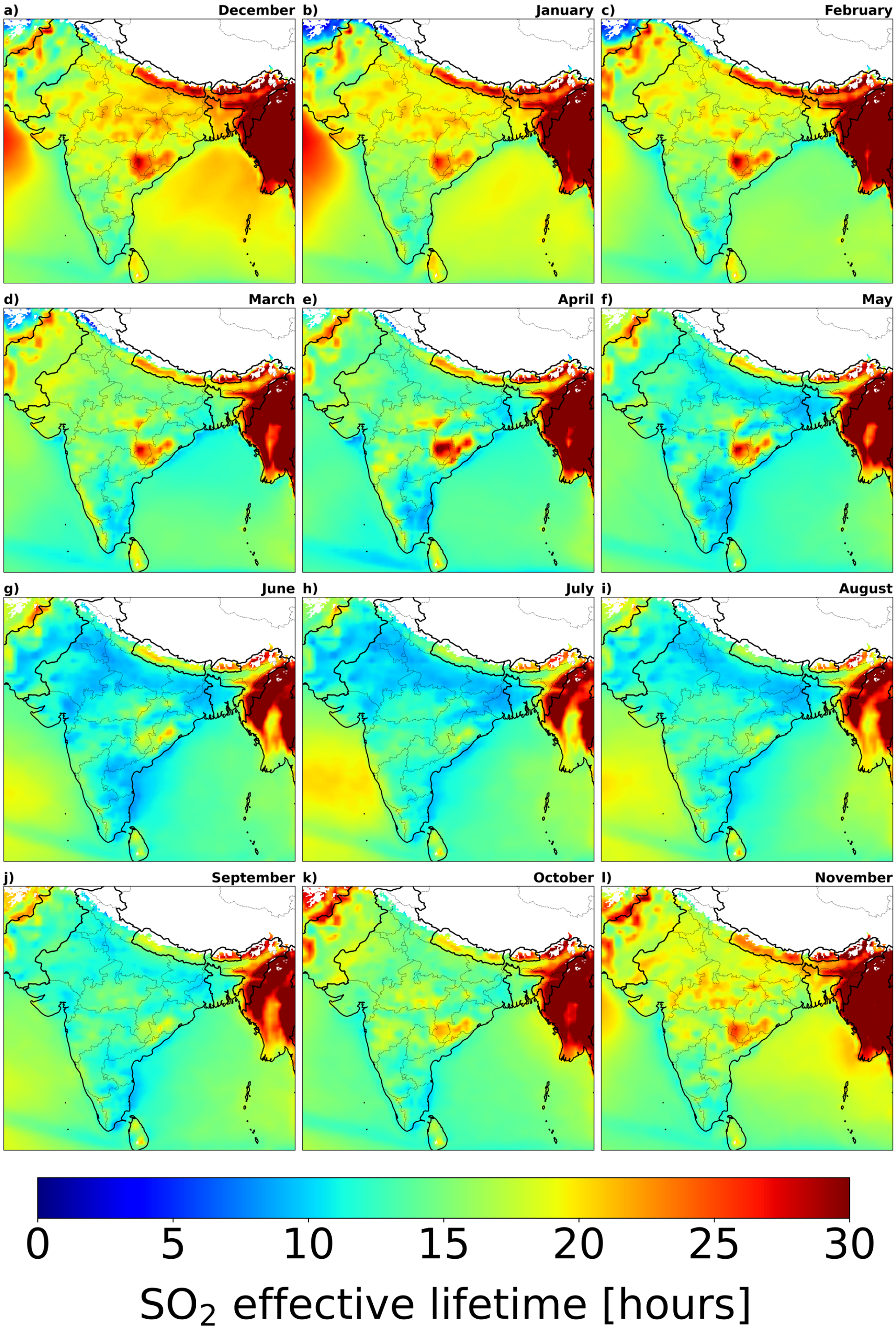

Figure S3. SO_2 monthly mean effective lifetime in India. The effective lifetime in each month is averaged within December 2018 to November 2023. The white region represents the areas with surface height above 3 km or the areas without high-quality SO2 measurements and are not discussed in this study.

5. SO_2 daily distribution in one-dimension

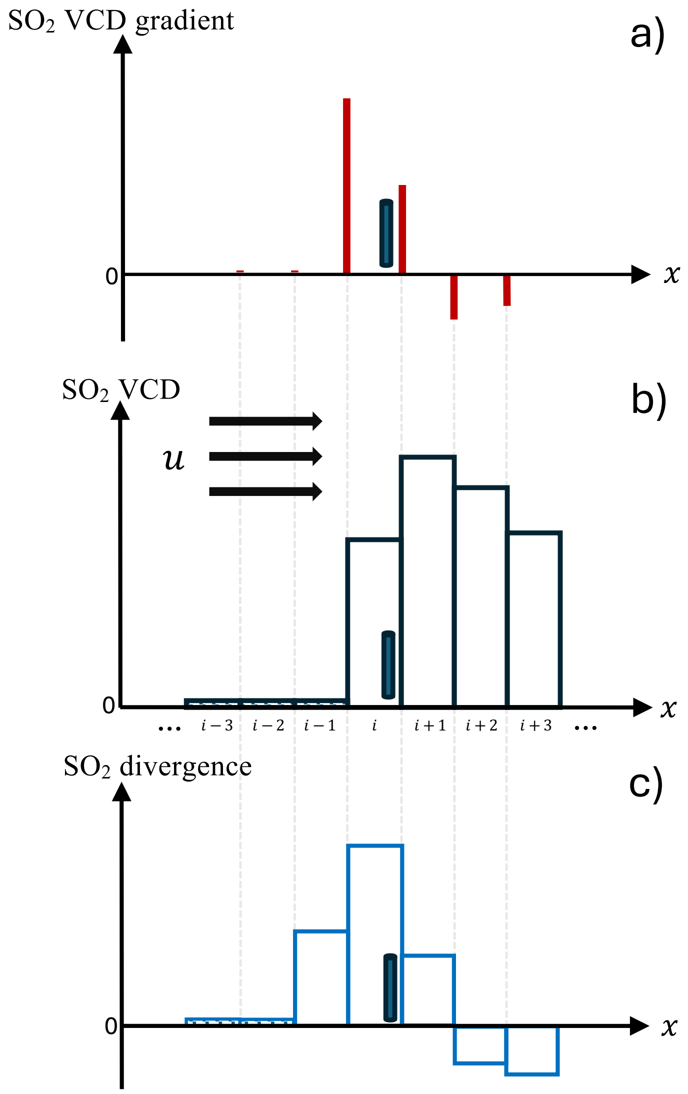

Figure S4. Illustration of a one-dimensional example of the (a) SO_2 concentration gradient, (b) daily SO_2 concentration and (c) the SO_2 divergence calculated with SOCFDM. The blue cylinder represents a point source of SO_2.

Formula of method A:

We set gradient of grid cell *i* ($Grad_{(i)}$) as:

$$Grad_{(i)} = V_{(i)} - V_{(i-1)}$$

When the divergence at the left edge of grid cell *i* ($D_{LE(i)}$) is needed to be allocated, we select between the gradient at the left side and at the right side of the edge, according:

If $\quad Grad_{(i+1)} > Grad_{(i-1)}$

Then $\quad D_{(i)} = D_{(i)} + D_{LE(i)}$

Else $\quad D_{(i-1)} = D_{(i-1)} + D_{LE(i)}$

When the divergence at the right edge of grid cell *i* ($D_{RE(i)}$) needs to be allocated:

If $$Grad_{(i)} > Grad_{(i+2)}$$

Then $$D_{(i)} = D_{(i)} + D_{RE(i)}$$

Else $$D_{(i+1)} = D_{(i+1)} + D_{RE(i)}$$

6. SO_2 daily concentration distribution in two dimensions

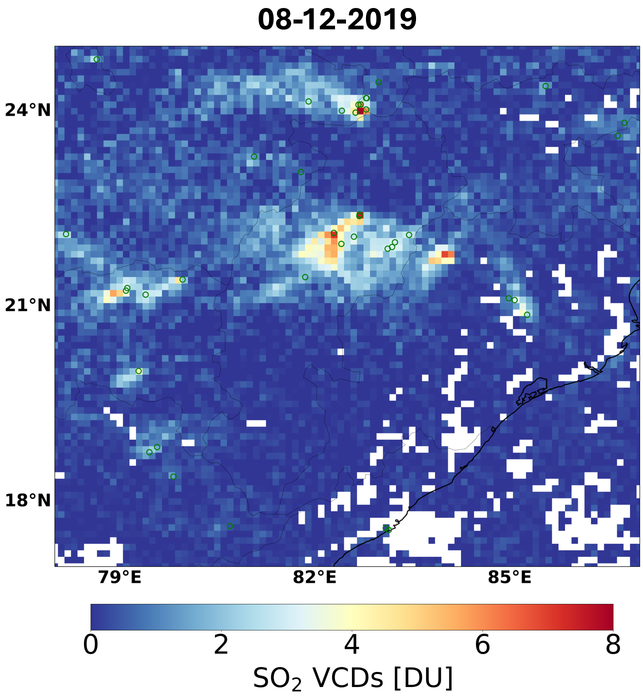

Figure S5. SO_2 daily VCDs on 8th December 2019. The green circles represent power plants.

Formula of method B:

When the divergence at the left edge of grid cell *i* ($D_{LE(i)}$) is needs to be allocated:

If $V_i > V_{i-1}$

Then $D_{(i)} = D_{(i)} + D_{LE(i)}$

Else $D_{(i-1)} = D_{(i-1)} + D_{LE(i)}$

which means always allocate the edge divergence to a grid cell with the larger SO_2 VCD.

7. Comparison between the emissions derived with method A and method B.

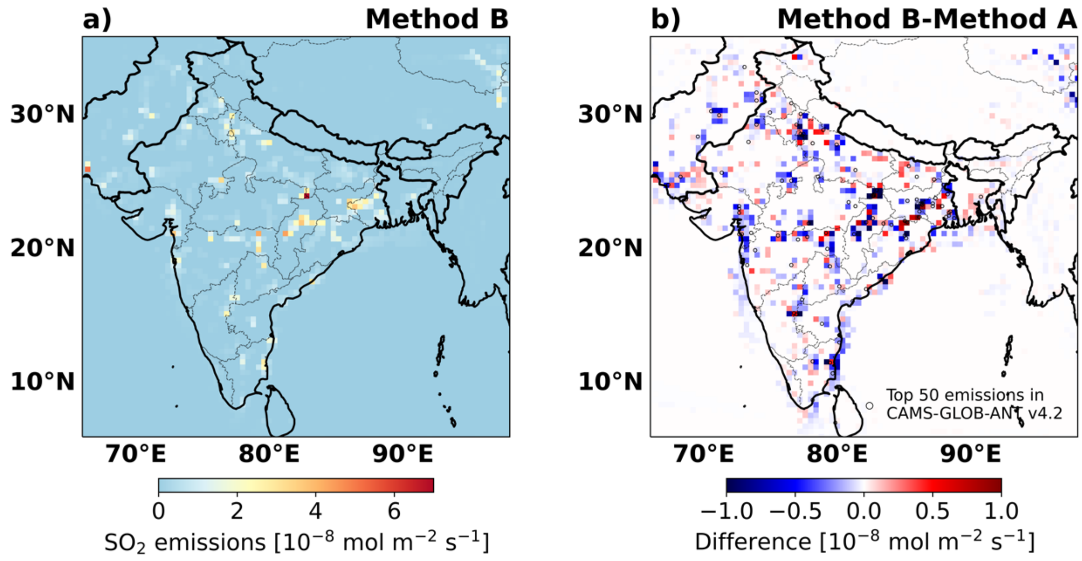

Figure S6. (a) The emissions derived with method B in the winter season (DJF) of 2019/2020 is shown. (b) The difference from emissions derived with method B and method A. The black circles represent the locations of the top 50 emission sources in the CAMS-GLOB_ANT v4.2 inventory.

8. Emissions detection threshold

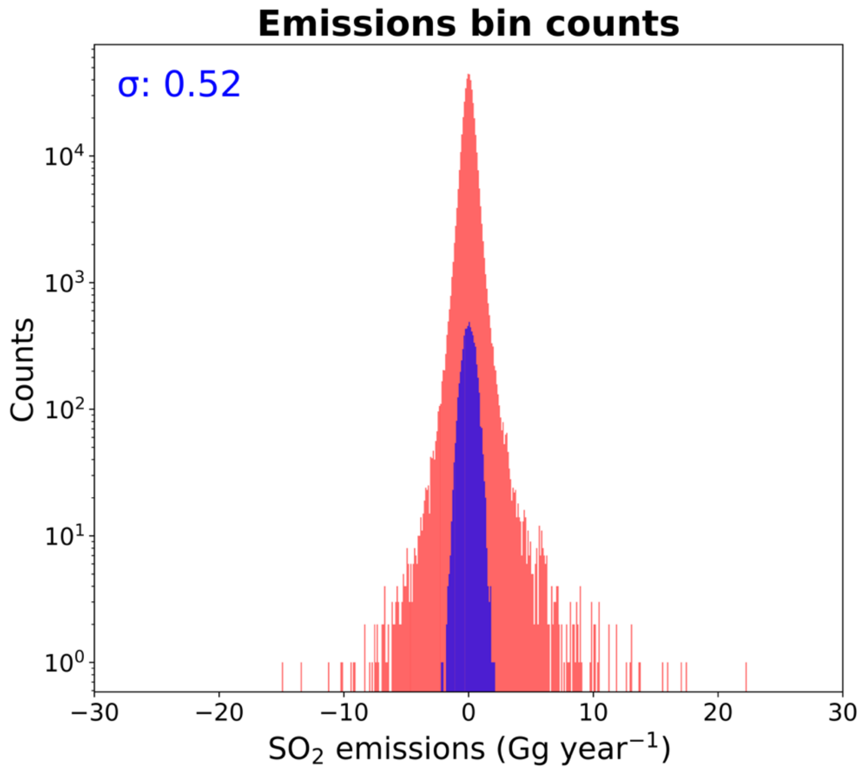

Figure S7. Histogram of the frequency of SO_2 emissions. The resolution of the bins is 0.1 Gg year^{-1}. The red bars represent the frequency of SO_2 emissions within the whole domain. The blue bars denote the frequency of SO_2 emissions (or the noise) in the selected clean oceanic region (latitude: 5°N-18°N; longitude: 85°E- 90°E), with $\sigma = 0.52$.

9. SO_2 emissions derived with fixed 6-hour lifetime

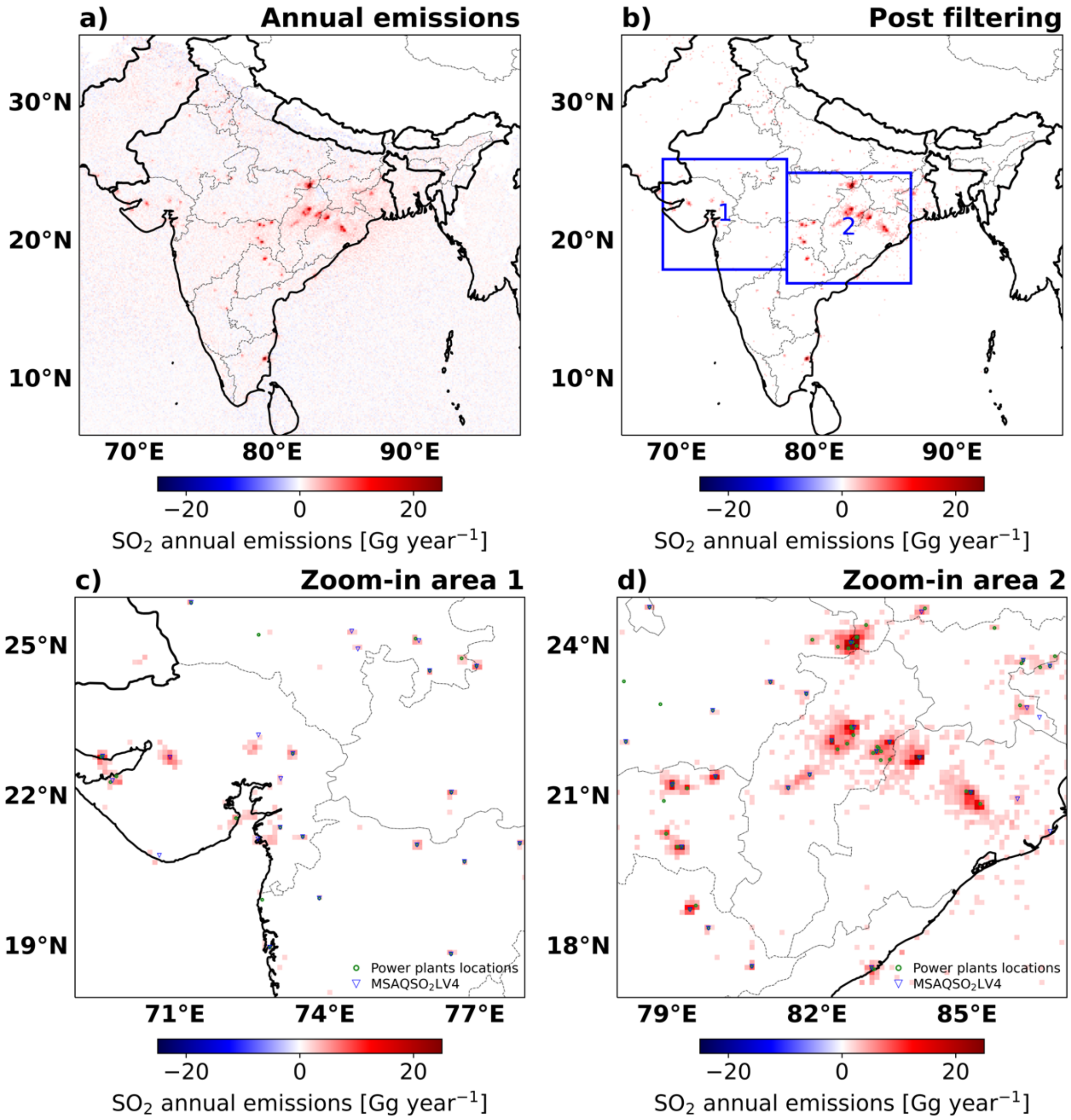

Figure S8. (a) The annual mean SO_2 emissions with a fixed 6-hour lifetime averaged within December 2018 to November 2023. (b) shows the emissions above the detection threshold of 2.0 Gg year^{-1}. (c) and (d) are the zoom-in areas. The blue triangles represent the source locations identified by the MSAQSO_2LV4 dataset. The green circles represent the locations of thermal power plants with annual power generation larger than 500MW.

10. Top 10 sources location

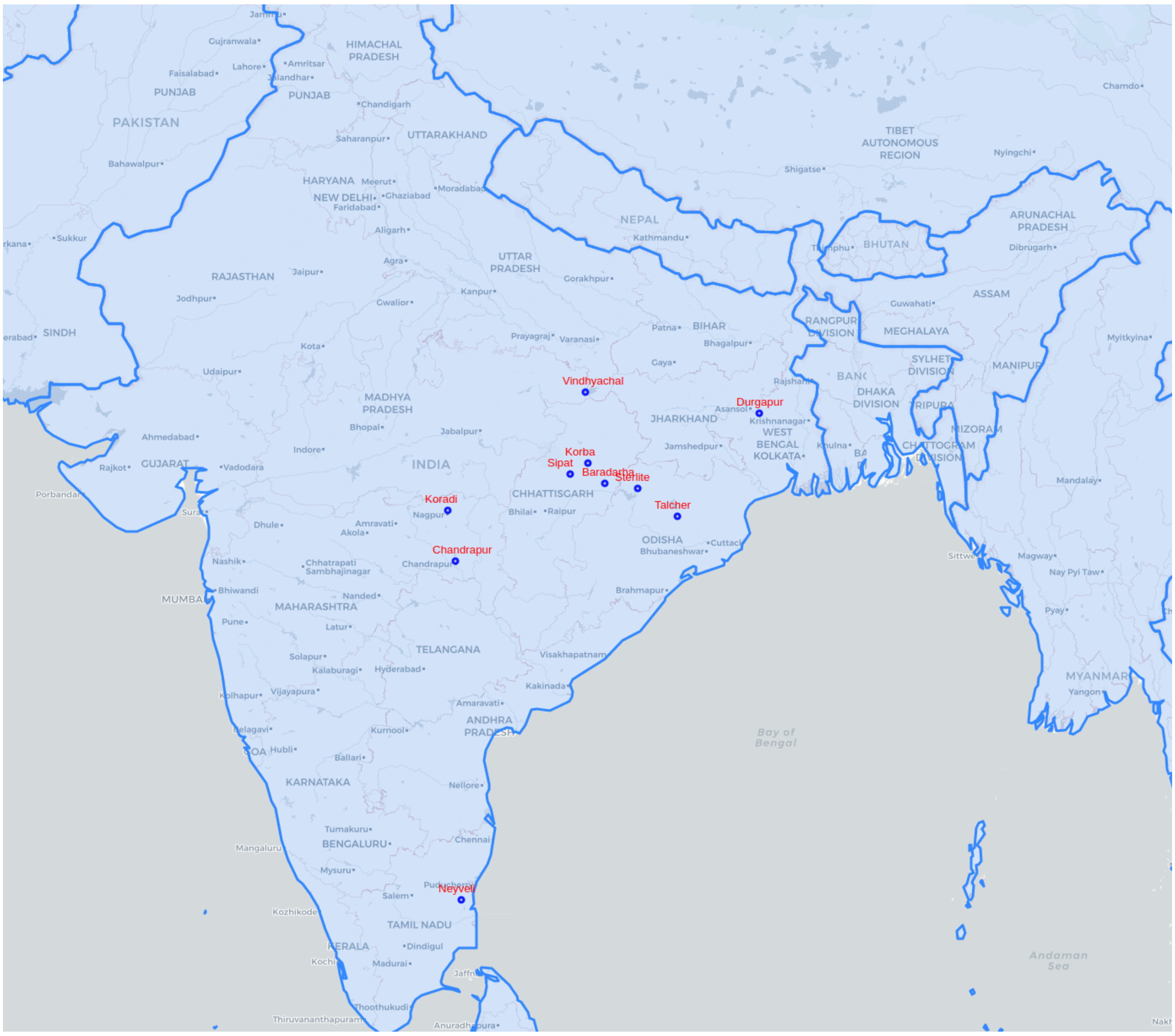

Figure S9. The locations of top 10 of highest emission sources in our inventory. (from © Google Maps 2024)

References:

Beirle, S., Borger, C., Dörner, S., Li, A., Hu, Z., Liu, F., Wang, Y., and Wagner, T.: Pinpointing nitrogen oxide emissions from space, Science Advances, 5, eaax9800, doi:10.1126/sciadv.aax9800, 2019.

Liu, M., van der A, R., van Weele, M., Eskes, H., Lu, X., Veefkind, P., de Laat, J., Kong, H., Wang, J., Sun, J., Ding, J., Zhao, Y., and Weng, H.: A New Divergence Method to Quantify Methane Emissions Using Observations of Sentinel-5P TROPOMI, Geophysical Research Letters, 48, e2021GL094151, https://doi.org/10.1029/2021GL094151, 2021.

Vladimir, O., James, B., Sander, S., J, D., Barker, J., Robert, H., Kolb, C., Michael, K., David, W., and Wine, P.: Chemical Kinetics and Photochemical Data for Use in Atmospheric Studies, Evaluation No. 18, 2015.